Using Artificial Neural Networks to Predict Seismic Shear-Induced Pore Water Pressure

[1, 2]Abdoullah Namdar
[1]*Research Consultant/ Department of Civil Engineering/ Abu Dhabi University/ UAE*
[2] Professor/*Structure Department/ Engineering Faculty/Afghan International Islamic University/ Kabul/ Afghanistan. ab-namdar@aiiu.edu.af*

[3]Omer Mughieda
[3]Associate Professor/*Department of Civil Engineering/ Abu Dhabi University/ Abu Dhabi/ UAE. omer.mughieda@adu.ac.ae*

ABSTRACT: The very loose sandy subsoil is observed in the UAE region. The high magnitude of the undrained cyclic shear stresses produced by the earthquake or explosion is a reason for liquefying the confined, low-permeable, saturated, noncohesive soil; this phenomenon is known as liquefaction. With minimizing liquefaction resistance and increasing the liquefaction zone of the sandy subsoil model, pore water pressure is raised, the sand particle contact is reduced, shear strength is immediately reduced, etc. This paper aims to predict the fluctuation of pore water pressure of the loose saturated sand by using the Artificial Neural Network (ANN) and advanced mathematical methods. The input for the ANN modeling was designed using the experimental data published in the literature. To establish the ANN model, acceleration history (g) is applied at a selected point, shear stress is applied at a designated point, and dynamic response of the model is used as input. The results indicate that using a suitable advanced method is an efficient technique to be used for predicting the fluctuation of the pore water pressure with minimized error.

1 INTRODUCTION

The pore water pressure is widely analyzed in predicting the soil seismic response and assessing the soil liquefaction resistance. However, a critical soil seismic response is associated with pore water pressure in the potential of liquefaction occurrence while impacting the mechanical properties of the soil and subsequently reducing the shear strength of the soil and developing unacceptable elastic differential settlement following nonlinear soil foundation deformation which ends with civil infrastructure different level of the damage lead to complete collapse (Namdar, 2016; Fourie et al., 2001; Seed, 1976; Pokhrel et al., 2024). In addition, unexpected cyclic pore water pressure fluctuation has remained a challenging topic in soil seismic design for predicting the liquefaction resistance considering the soil permeability in the drainage mechanism of the soil, and the initial density of the soil (Cao et al., 2011; Zhou et al., 2024). Some natural minerals such as calcite even in small quantities contaminated in the sand improve the liquefaction resistance (O'Donnell et al., 2017), also, the lower sand saturation level makes suspensions in the development of excess pore pressure (Lv et al., 2024). With the complicated behavior of the excess pore water pressure, need to enhance monitoring of the pore water pressure prediction that can be applied to any soil situation.

The sensors and high-speed images have been employed, to monitor the fluctuation of pore water pressure causes dynamic and static liquefaction (Steers et al., 2024; Namdar and Khodashenas Pelko, 2011). Several laboratory and field-based semi-empirical methods are applied to liquefaction assessment. It is complicated to apply relative density to unclean sand for liquefaction prediction. The problems extend to applying laboratory and empirical methods on silts, silty sands, gravelly sands, and sandy gravels (Cubrinovski, 2019). The damage on the sand subjected to liquefaction may be reduced from strain-softening to strain-hardening in controlling pore water pressure and enhancing the liquefaction resistance (Peng et al., 2018; Peng et al., 2021a; Peng et al., 2021b). The pore water pressure also impacts the settlement of the sandy foundation (Marasini and Okamura, 2015). It is important to predict the pore water pressure of a sandy subsoil that is subjected to liquefaction using advanced methods.

The mathematical advanced method needs to be applied for solving geotechnical problems when the experimental and numerical modeling do not provide sufficient conclusions (Namdar, 2020a;

Namdar, 2020b). The fluctuation of the excess pore pressure ratio has been predicted to improve the liquefaction resistance in the sand using artificial neural networking (ANN) and advanced mathematical methods. Also, the exact pore water pressure predicted to realize the liquefaction resistance of the saturated sand subjected to cyclic loading.

2 METHOD AND MATERIAL

In most of the applications of the ANN, an overview of the prediction for outcome models has been presented in the literature (Namdar, 2020a; Guo et al., 2021). The excess pore water pressure occurs in the soil foundation during applying cyclic loading to the model. ANN is based on all data to provide the appropriate prediction for realizing scientific problems.

This prediction in ANN is based on all data, it is possible to predict every single value for the shear strength and pore water pressure of the model. The exact prediction of the shear strength and pore water pressure significantly supports realizing the liquefaction mechanism in the model. To evaluate the relationship between a set of experimental results that is available in the literature the ANN was applied to enhance prediction quality.

The input for the ANN modeling was designed using the experimental data published in the literature (Gopalakrishna and Namdar, 2009). In ANN architectural design 60%, 20%, and 20% of data for training, validation, and testing and a single hidden layer have been proposed. To establish the ANN model, acceleration history (g) is applied at a selected point, shear stress is applied at a designated point, and the dynamic response of the model is used as input. The prediction accuracy of the ANN concerns the pore water pressure value. To identify liquefaction resistance the single value of the pore water pressure was identified in the negative and positive directions of the applying cyclic loading. In addition, an overview of the prediction was presented.

ANN applied for modeling of unconfined compressive strength of soil that impacted to the heavy metal (Jaffar et al., 2024), reinforced soil foundations behaviour prediction (Amjad Raja et al., 2024) and predict the settlement mechnism of geosynthetic-reinforced soil (Amjad Raja et al., 2021).

3 PORE WATER PRESSURE

The pore water pressure of the simulated sand has been reported in the literature (Gopalakrishna and Namdar, 2009). Based on several uncontrollable factors impact the experimental and numerical results. In most experimental work and numerical simulations, enhancement investigation results are one of the key factors in developing suitable conclusions for strengthening the literature and applying findings to solve scientific problems (Namdar, 2016; Namdar and Khodashenas Pelko, 2011; Namdar, 2020c). The pore water pressure of the loose saturated sand needs to be investigated in detail with attention to the quality improvement of the results.

The soil was undrained loose sand subjected to a loading frequency of 0.1 Hz. The failure of sand occurred with a loose sample simulated (D_r = 35 % and CSR = 0.13). The experimental results were compared with the numerical simulation outcome to validate the investigation (Gopalakrishna and Namdar, 2009). This experimental result has been used to predict the pore water pressure using ANN and advanced mathematical methods. According to the excess pore water pressure mechanism in cyclic applied load, the cyclic mode is cumulative of pore water pressure in plastic deformation of the loose sand model. Increasing the cyclic number of the dynamic loading changes the loose sand liquefaction resistance and leads to excess pore water pressure.

Figure 1 illustrates the embankment and subsoil model. The acceleration was applied in the base model. The model's excess pore water pressure (kPa) was recorded by sensors P1, P2, P3, and P4. The model's acceleration time history (m/s^2) was recorded by sensors A1, A2, and A3. Figures 2 and 3 illustrate the model's excess pore water pressure (kPa) and the model's acceleration time history (m/s^2) respectively.

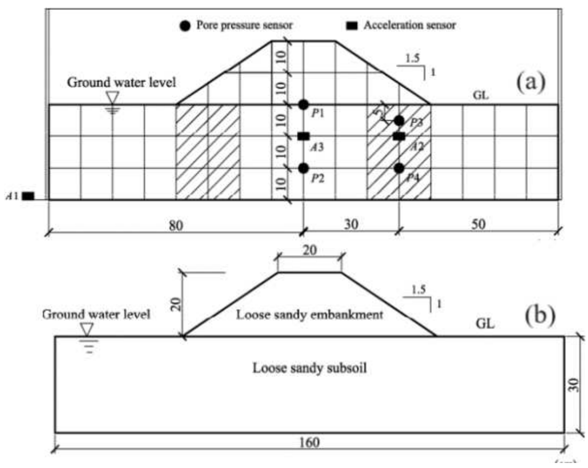

Fig. 1. The model setup under cyclic loading (Gopalakrishna and Namdar, 2009).

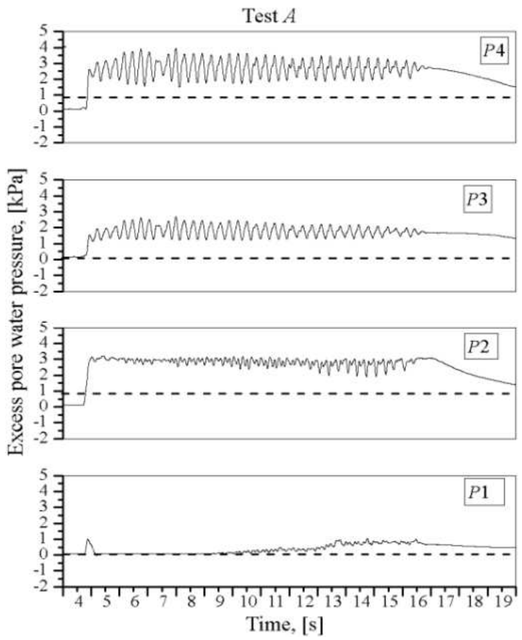

Fig. 2. The model's excess pore water pressure (kPa) under cyclic loading (Gopalakrishna and Namdar, 2009).

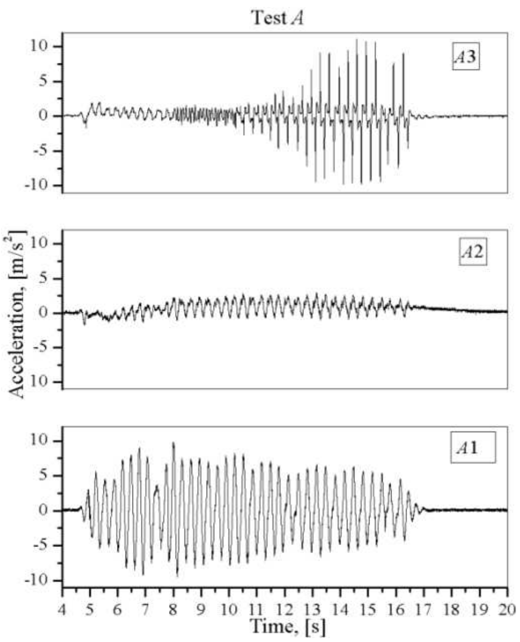

Fig. 3. The model's acceleration time history (m/s²) under cyclic loading (Gopalakrishna and Namdar, 2009).

4 PREDICTION OF THE PORE WATER PRESSURE

The prediction of the pore water pressure values in the negative and positive directions of the applying cyclic loading is presented in Figure 2. ANN predicts the pore water pressure with overall accuracy. The significantly modified excess pore water pressure is observed at a certain peak of cyclic shearing. The select part of the excess pore water pressure (kPa) model under cyclic loading has been shown in Figures 4 and 5. From 9 (s) to 12 (s) excess pore water pressure (kPa) has been selected for investigation.

Based on the model's excess pore water pressure (kPa) under cyclic loading from the literature (Gopalakrishna and Namdar, 2009), the results presented in Table 1 were used in the prediction process.

Figure 4 shows prediction results for the excess pore water pressure (kPa) using experimental, Spline, ANN, and Spline methods. In this method, the correction of the result is not significant. Figure 5 shows the prediction of excess pore water pressure (kPa) by applying experimental, Spline, ANN, and B-Spline methods. The B-Spline significantly changes the excess pore water pressure (kPa) prediction. Figure 6 shows the best validation performance for predicting excess pore water pressure (kPa). According to ANN, the R^2 for training, validation, and testing are 0.77, 0.77, and 0.76 respectively. And MSE for training, validation, and testing are 4.28, 4.55, and 3.92 respectively.

The magnitude of effective stress continuously decreases as the increment of pore water pressure on the simulated model, and a big residual deformation is developed after the application of the number of cycles (Yanga and Pan, 2017), this category of sand failure mechanism can be called residual deformation failure (Chiaro et al., 2012). Due to applying undrained cyclic loading on sandy soil, the model exhibits a reduction in strength, and nonlinear deformation leads to the liquefaction status following the buildup of excess pore water pressure and the reduction of stress-strain hysteretic loops has been observed (Namdar and Gopalakrishna, 2009). The generation and reduction of the pore water pressure in the prediction process have been modified. These outcomes improve the explanation of the deformation and failure modes of the model with higher accuracy.

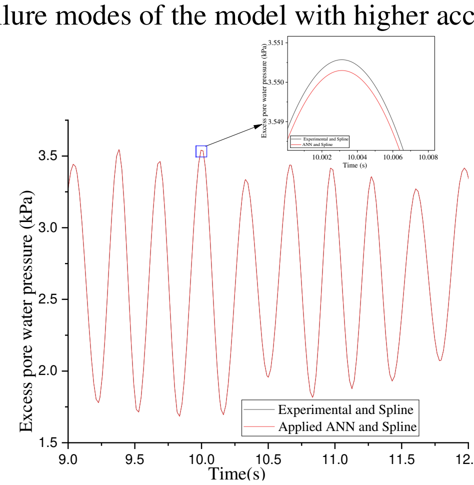

Fig. 4. Excess pore water pressure (kPa) from experimental, Spline, ANN, and Spline.

Table 1. Data from the experimental was used in ANN.

Time (s)	Predominant frequency, [Hz] for A1	Pore water pressure increasing rate [kPa] for P4	Pore water pressure dissipation rate [kPa] for P4	Excess pore water pressure (kPa) for P4	Acceleration time history (m/s^2) for P4	Excess pore water pressure (kPa) for P4 from ANN
8.89611	3.21	1.92	0.39	7.3755	1.91653	1.9165
9.06754	3.21	1.92	0.39	-7.70504	3.37591	3.37591
9.23897	3.21	1.92	0.39	6.85357	1.81657	1.81644
9.38511	3.21	1.92	0.39	-7.02764	3.53584	3.5357
9.51158	3.21	1.92	0.39	6.28721	1.73161	1.73145
9.69144	3.21	1.92	0.39	-6.98322	3.45587	3.45595
9.8179	3.21	1.92	0.39	7.65312	1.71162	1.71164
10.01182	3.21	1.92	0.39	-7.94935	3.53584	3.53557
10.14671	3.21	1.92	0.39	7.97517	1.73161	1.73163
10.32939	3.21	1.92	0.39	-7.46073	3.33592	3.33602
10.50082	3.21	1.92	0.39	8.00848	1.95651	1.9565
10.67225	3.21	1.92	0.39	-7.58289	3.43588	3.43576
10.84087	3.21	1.92	0.39	5.68754	1.83656	1.8365
10.96733	3.21	1.92	0.39	-6.18366	3.41589	3.41595
11.12752	3.21	1.92	0.39	6.77583	1.87655	1.87662
11.27366	3.21	1.92	0.39	-7.26084	3.35592	3.35584
11.41137	3.21	1.92	0.39	6.88688	1.9765	1.97658
11.60528	3.21	1.92	0.39	-6.2614	3.27095	3.27101
11.79638	3.21	1.92	0.39	6.05401	2.07646	2.07642
11.93409	3.21	1.92	0.39	-6.06151	3.31093	3.31093
12.13924	3.21	1.92	0.39	5.04346	1.95651	1.95618

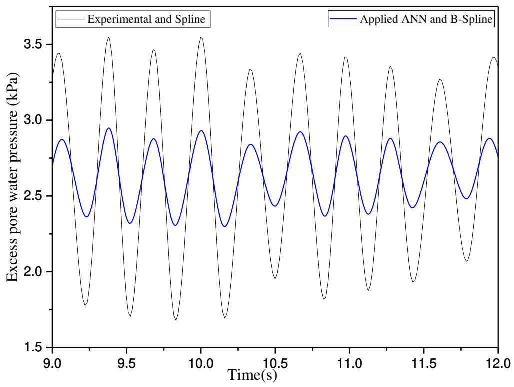

Fig. 5. Excess pore water pressure (kPa) from experimental, Spline, ANN, and B-Spline.

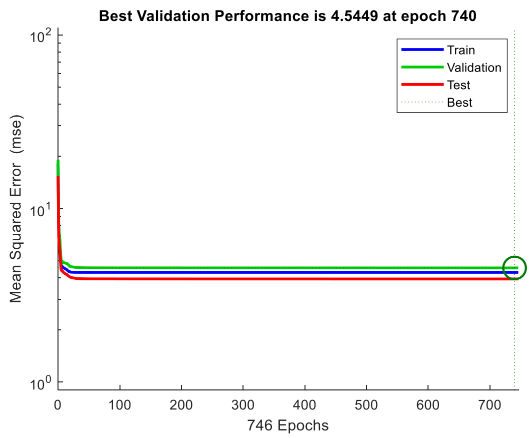

Fig. 6. The best validation performance for predicting excess pore water pressure (kPa).

5 LIQUEFACTION

The loose saturated sand response to a strong load leads to excess pore water pressure and causes liquefaction (Rehman et al., 2022), the liquefaction reaches a high level and results in a catastrophic phenomenon when the drainage paths of the soil are fully blocked, and the impermeable soil increases the cyclic loading impact in producing of the liquefaction (Shen et al., 2022). The liquefaction types are associated with the failure mode of the loose saturated sand subjecting to cyclic loading. The liquefaction resistance may increase or decrease concerning several factors. If liquefaction resistance increases further cyclic shearing stress is needed for liquefaction occurrence following unallowable nonlinear deformation.

6 SHEAR STRENGTH

Generally, the excess pore water pressure causes a reduction in the shear strength of the loose saturated sand in dynamic analysis. Excess pore water pressure causes a high reduction in the sand particles' contact and reduces liquefaction resistance. The shear strength of the loose saturated sand impacts the seismic stability and nonlinear deformation of the structure resting on the soil foundation. The shear strength of sand has a direct relationship to the deformation and settlement. The excess pore water pressure reduces the density of the loose sand. This phenomenon results in a decrease in the shear strength. The minimum level of the shear strength is expected with the peak of the pore water pressure. The ANN helps to identify the fluctuation mechanism of the pore water pressure. To realize the shear strength behavior of the sand needs to consider the pore water pressure mechanism. The highest nonlinearity of the pore water pressure may cause the maximum nonlinear deformation and settlement.

7 DIFFERENTIAL SETTLEMENT

The differential settlement of the sandy soil subjected to cyclic loading reduces when the saturation degree of the sand reduces (Lv et al., 2024). The impact of liquefaction on building damage increases when the building rests on a shallow foundation (Lashkari et al., 2017). The surcharge may impact liquefaction and control the liquefaction. Large differential settlement of loose saturated sand after the soil liquefaction is the main reason for seismic damage. The infrastructure collapse occurs due to the high magnitude of the differential settlement. Based on the prediction of the pore water pressure fluctuation the mechanism of the differential settlement may be changed in both negative and positive directions of simulated applied seismic loading.

The seismic stability of the structure is associated with the magnitude of nonlinear settlement and deformation of the soil foundation. In addition, the nonlinear settlement is a reason for developing cracks in the building and infrastructure. Improve prediction quality of the differential settlement helps in the crack occurrence on the buildings and infrastructure.

This study concentrated on the experimental data available in the literature, the assumption made with parameters impact to the soil available in the literature. The soil has a complicated seismic response due to the function of the unknown parameters that impact the strength and stiffness of the soil.

Inadequate data can be predicted by using ANN. In the application of ANN to predict the liquefaction index, in the architectural design of ANN, the good quality input data significantly influences results. In addition, the ANN integrates the experimental results. ANN could provide the predicted data that is difficult or expensive by experiment.

In earthquake geotechnical engineering, loose saturated sands frequently encounter cyclic loading in the seismic zone, which may be subjected to simple shear loading conditions that could enhance the density quality of soil and improve liquefaction resistance. The irregular cyclic shear stress in acceptable magnitude enhances the mechanical properties of the loose saturated soil. The excess pore water pressure controls liquefaction resistance and nonlinear settlement. The ANN is applicable in the prediction of liquefaction resistance and nonlinear settlement with data used in the prediction of excess pore water pressure mechanism.

8 CONCLUSION

The pore water pressure fluctuation in the loose saturated sand has been predicted using ANN. The shear strength of the loose saturated sand was discussed. The data for investigation has been used from those available in the literature.

The level of prediction accuracy is acceptable with the application of mixed suitable methods on the experimental results.

The outcome of the present investigation supports the realization of liquefaction resistance of loose saturated sand in acceptable quality.

The level of the loose saturated sand has not been considered in the recent investigation. This topic can be a research topic for future research work.

The soil seismic stability and liquefaction potential index prediction is a challenging issue in geotechnical earthquake engineering. The fluctuation liquefaction potential mechanism is predictable by using an ANN model in engineering acceptable quality.

This study assumes that all parameters governing the liquefaction are realized. The limitations associated with applying ANN in liquefaction index modeling need exploration in advance for future work. The limitations of the investigation are associated with unknown parameters governing the liquefaction index.

ACKNOWLEDGEMENTS

The authors are grateful for the financial support provided by Abu Dhabi University. The project presented in this paper is supported by an internal Abu Dhabi University grant.

REFERENCES

Amjad Raja, M.N. and Kumar Shukla, S. (2021). Predicting the settlement of geosynthetic-reinforced soil foundations using evolutionary artificial intelligence technique. Geotextiles and Geomembranes. Vol. 49(5): pp. 1280-1293. https://doi.org/10.1016/j.geotexmem.2021.04.007

Amjad Raja, M.N., Abdoun, T. and El-Sekelly. W. (2024). Exploring the Potential of Machine Learning in

Stochastic Reliability Modelling for Reinforced Soil Foundations. Buildings, Vol. 14(4): PP. 954. https://doi.org/10.3390/buildings14040954

Cao, Z., Leslie Youd, T. and Yuan, X. (2011). Gravelly soils that liquefied during 2008 Wenchuan, China earthquake, Ms=8.0. Soil Dynamics and Earthquake Engineering, Vol. 31(8): 1132-1143. https://doi.org/10.1016/j.soildyn.2011.04.001.

Chiaro, G., Koseki, J. and Sato, T. (2012). Effects of initial static shear on liquefaction and large deformation properties of loose saturated Toyoura sand in undrained cyclic torsional shear tests. Soils and Foundations, 52(3): pp. 498-510. https://doi.org/10.1016/j.sandf.2012.05.008

Cubrinovski, M. (2019). Some important considerations in the engineering assessment of soil liquefaction. NZ Geomechanics News, Vol. 97: pp,19-36.

Fourie, A., Blight, G. and Papageorgiou, G. (2001). Static liquefaction as a possible explanation for the Merriespruit tailings dam failure. Canadian Geotechnical Journal, Vol. 38 (4): pp. 707-719. https://doi.org/10.1139/t00-112.

Gopalakrishna, G.S. and Namdar, A. (2009). Stability analysis of the embankment model. Bulletin of the Polytechnic Institute of Jassy, Universitatea Tehnică, Gheorghe Asachi, din Iaşi. Tomul LV (LIX), Fasc. 4, Secţia, Construcţii Ărhitectură.

Guo, L., Li, W., Namdar, A. (2021). Using recycled aggregate for seismically monitoring of embankment-subsoil model. Case Studies in Construction Materials,15: e00605. https://doi.org/10.1016/j.cscm.2021.e00605

f

Lashkari, A., Karimi, A., Fakharian, K. and F. Kaviani-Hamedani, F. (2017). Prediction of undrained behavior of isotropically and anisotropically consolidated firoozkuh sand: instability and flow liquefaction. International Journal of Geomechanics, 17 (10): 04017083. https://doi.org/10.1061/(ASCE)GM.1943-5622.0000958

Lv, M., Zhang, D. and Xu, T. (2024). Seismic response of mitigation of sand liquefaction beneath existing buildings using microbial induced desaturation. Case Studies in Construction Materials, 20: e02926. https://doi.org/10.1016/j.cscm.2024.e02926.

Marasini, N.P., Okamura, M. (2015). Numerical simulation of centrifuge tests to evaluate the performance of desaturation by air injection on liquefiable foundation soil of light structures, Soils and Foundations, 55 (6): pp.1388-1399. https://doi.org/10.1016/j.sandf.2015.10.005

Namdar, A. (2016). Liquefaction Zone and Differential Settlement of Cohesionless Soil Subjected to Dynamic Loading. EJGE, Vol. 21. Bund. 02: 593- 605.

Namdar, A. (2020a). The forecasting bearing capacity of the mixed soil using artificial neural network. Frattura ed Integrita Strutturale, 53: pp. 285-294. https://doi.org/10.3221/IGF-ESIS.23.22

Namdar, A. (2020b). The application of soil mixture in concrete footing design using linear regression analysis. Material Design & Processing Communications (MDPC), e179. https://doi.org/10.1002/mdp2.179

Namdar, A. (2020c). The multilayered soil-structure seismic interaction and structure vibration mechanism. Frattura ed Integrità Strutturale, 51: pp. 267-274. https://doi.org/10.3221/IGF-ESIS.51.21

Namdar, A. and Gopalakrishna, G.S. (2009). Seismic Mitigation of Embankment by Using Dense Zone in Subsoil, Emirates Journal for Engineering Research, 13 (3): pp. 55-61.

Namdar, A. and Khodashenas Pelko, A. (2011). Embankment loading analysis in laboratory condition. INGENIERÍA E INVESTIGACIÓN, Vol. 31(2): pp. 48-51.

O'Donnell, S.T., Rittmann, B.E. and Kavazanjian Jr, E., (2017). MIDP: Liquefaction mitigation via microbial denitrification as a two-stage process. I: Desaturation. J. Geotech. Geoenvironmental En, Vol. 143: 04017094. https://doi.org/10.1061/(ASCE)GT.1943-5606.0001818

Peng, E., Hou, Z., Sheng, Y., Hu, X., Zhang, D., Song, L. and Chou, Y. (2021b). Anti-liquefaction performance of partially saturated sand induced by biogas under high intensity vibration. Journal of Cleaner Production, 319: 128794. https://doi.org/10.1016/j.jclepro.2021.128794

Peng, E., Sheng, Y., Hu, X., Zhang, D. and Hou, Z. (2021a). Mitigation of sand liquefaction under static loading condition using biogas bubbles generated by denitrifying bacteria. Journal of Environmental Management, 295: 113106. https://doi.org/10.1016/j.jenvman.2021.113106

Peng, E., Zhang, D., Sun, W. and Du, G. (2018). Desaturation for liquefaction mitigation using biogas produced by Pseudomonas stutzeri. Journal of Testing and Evaluation, Vol. 46 (4): 20170435. https://doi.org/10.1520/JTE20170435

Pokhrel, A., Chiaro, G., Kiyota, T. And Cubrinovski, M. (2024). Liquefaction characteristics of sand-gravel mixtures: Experimental observations and its assessment based on intergranular state concept. Soils and Foundations, Vol. 64(2): 101444. https://doi.org/10.1016/j.sandf.2024.101444.

Rehman, Z., Khalid, U., Ijaz, N., Mujtaba, H., Haider, A., Farooq, K. and Ijaz, Z. (2022). Machine learning-based intelligent modeling of hydraulic conductivity of sandy soils considering a wide range of grain sizes. Engineering Geology. 311: 106899. https://doi.org/10.1016/j.enggeo.2022.106899

Seed, H.B. (1976). Evaluation of soil liquefaction effects of level ground during earthquakes. Presented at the ASCE Annual Convention and Exposition, Philadelphia.

Shen, J., Bao, X., Cui, H., Chen, X. (2022). Experimental investigation on the relationship between influence factors of liquefaction and microstructural characteristics of muddy sand. Construction and Building Materials. 324: 126619. https://doi.org/10.1016/j.conbuildmat.2022.126619

Steers, L.J., Beddoe, R.A. and Take, W.A. (2024). Propagation velocity of landslide-induced liquefaction and entrainment of overridden loose, saturated sediments. Engineering Geology, 334: 107523. https://doi.org/10.1016/j.enggeo.2024.107523.

Yanga, Z.X. and Pan, K. (2017). Flow deformation and cyclic resistance of saturated loose sand considering initial static shear effect. Soil Dynamics and Earthquake Engineering, 92: pp. 68-78. https://doi.org/10.1016/j.soildyn.2016.09.002

Zhou, Xi.H., Zhou, Y.G. and Chen, Y.M. (2024). The failure type-dependent characterization of liquefaction resistance by small-strain shear modulus for saturated sand. Engineering Geology, Vol. 335: 107526. https://doi.org/10.1016/j.enggeo.2024.107526.